

A rigorous solution for electromagnetic scattering from any kind of asperities of multilayer 1-D structures in the X-ray–VUV ranges

Leonid I. Goray*

Institute for Analytical Instrumentation, Russian Academy of Sciences, Rizhsky Pr. 26, St.
Petersburg, 190103 Russia

ABSTRACT

The rigorous integral equation method (viz MIM) in which the border structure is represented by a multilayer 1-D grating working at small wavelength-to-period ratios is used for taking into account electromagnetic scattering from different-types of nano-irregularities, such as periodical, random, self-organized, and their combinations. An example of the third type is multiple quantum dot (QD) ensembles and quantum molecules. The borders may contain a few or a large number of asperities of any kind. The program deals with a structure that is a grating from a mathematical point of view but that can model a rough surface if the groove spacing becomes large compared with the width (or correlation length) of asperities. This classical model for scattered light computation of bulk or few-border rough mirrors and gratings at visible and IR wavelengths is applied in PCGrate®-SX v.6.2 software based on the MIM to calculate multilayer structures in the X-ray–VUV range, which is a very difficult problem for any rigorous method, even for 1-D surfaces. Border profiles of most realistic types including real ones (e.g. AFM-measured) have both periodical and random components, and some ensemble averaging is required to obtain exact specular and nonspecular (diffuse) scattering intensities. The PCGrate results are compared with the data obtained by approximated approaches and measurements. Calculated intensities of scattering from gratings and rough mirrors as well as multiple QD structures can differ from those obtained for ideal and average border profiles or from approximations by a few percent up to a few orders of magnitude. The method can be applied both to forward computations of efficiencies over a wide range of angles and to fitting of the border metrological performance by comparing to measured data.

Keywords: X-ray–VUV metrology, specular and nonspecular scattering, X-ray reflection, diffraction gratings, rough multilayers, quantum dot ensembles, rigorous electromagnetic theory, boundary integral equations, grating efficiency modeling, PCGrate® software

1. INTRODUCTION

Rigorous methods of analysis, the most universal and, at the same time, the most difficult approach to development of an algorithm and obtaining numerical results, are used for diffraction gratings of various kinds and non-periodic corrugated structures, as there is actually no other alternative. These methods offer a rigorous way to gaining information on the scattered field which cannot be obtained with asymptotic techniques such as the Kirchhoff approximation or small-perturbation methods. To solve Maxwell's equations without invoking approximations, excluding those needed for discretization and truncation, one would have to tackle the problem of scattering by irregularities of any type having an rms height and/or correlation length (width) of the same order of magnitude as the wavelength. Even for today's computers, rigorous computation of the field scattered off rough surfaces is one of the most difficult problems to handle in electromagnetism and optics. The one-dimensional surface problem (i.e., the case of cylindrical surfaces) cannot be considered in a general way, because one has to deal in this case with multi-boundary surfaces having a large number of large asperities illuminated at grazing incidence and with short wavelengths.

Among the large variety of exact theoretical approaches and their modifications used for calculation of diffraction grating efficiency and scattered light intensity, the boundary integral equation method occupies a particular place.

*lig@skylink.spb.ru; phone 7-812-251-0956; fax 7-812-251-7038; www.iai.rssi.ru/en/index.php

Integral methods are intended to yield the total field and/or its normal derivative on the surfaces; these surface unknowns are linked to the incident field through integral equations, and the method of moments (collocation) transforms these equations to a linear system. It was one of the first numerical methods capable of providing a solution to problems of practical importance encountered with periodic and non-periodic structures [1-3]. One should add that despite intense development of other rigorous methods [4-6], boundary integral equations remain a universal and powerful tool in diffraction research as applied to gratings and mirrors of all types over an extremely broad spectral range [7-12]. In many important cases, the integral equation approach is thus far the only way acceptable from the practical point of view and capable of providing accurate predictions of diffraction features [13-16].

The PCGrate® software [17] is based on a modified method of boundary integral equations (MIM) [9, 15, 18]. The PCGrate programs enable the user to accurately solve the periodic boundary value problems which describe the incidence of a light beam on the relief or phase diffraction grating or mirror. Our software is indispensable for efficiency calculations of diffraction problems in the shortest wavelength range, from hard X-rays to VUV, due to the optimization of the number of plus and minus terms in Green's functions and their normal derivative expansions, an extended approach to the accounting of single-term corrections, and various refinements at the algorithmic level. PCGrates are especially convenient and accurate for efficiency modeling with a real groove profile function. A particularly revealing illustration to this is the case of border profiles determined by: atomic-force microscopy (AFM), transmission electron microscopy (TEM), micro-interferometry, stylus profilometry, as well as by indirect methods like actual scattering measurements or modeling, etc [11, 15, 19-20].

Further progress in the investigation of random atomic-scale roughness in multilayers and of self-assembled structures such as quantum dots (QDs) or other low-dimensional surface irregularities with typical sizes on the order of 10-nm or even less and having unique optoelectronic properties requires development of methods that would provide more accurate characterization of structural details [21]. Non-destructive X-ray reflection generally has the potential to investigate the fine structure of such complex samples. However, multiple and multi-wave diffraction, refraction, absorption, and resonances influence significantly X-ray scattering from nano-irregularities, and these effects are taken into account by present theories only approximately. The MIM employed in the analysis of diffraction by gratings is extended here to the case of 1-D non-periodical and quasi-periodical structures of any kind. The software developed (viz PCGrates-S(X) v.6.2) allows one to operate with exact models based on Maxwell's equations, exact boundary conditions, and radiation conditions. The present report dwells on an application of a comprehensive numerical analysis of X-ray scattering from multi-boundary surfaces having asperities of different shapes, lateral and vertical correlation lengths, surface densities, and fractal dimensions, with the use of a low- or mid-end workstation in a reasonable computation time.

2. MODELS OF A ROUGH SURFACE

The height probability distribution of a rough surface is often taken to be Gaussian. If the profile of a surface derives from a large number of local independent events whose effects are cumulative (such as the formation of evaporated thin films), the resultant height will obey nearly Gaussian statistics. The Gaussian height distribution function is

$$p(y) = (1/\sigma\sqrt{2\pi}) \exp\{-(y - y_0)^2/2\sigma^2\} \quad (1)$$

where σ is the rms height of the surface (variance).

Gaussian variates have the remarkable property that the random process is entirely determined by the height probability distribution and the autocorrelation function $C(y)$. The correlation function plays a fundamental role in the surface aspect. The frequently used form of the correlation function may also be Gaussian so that

$$C(y) = \sigma^2 \exp\{-(y - y_0)^2/L^2\}. \quad (2)$$

The correlation length L identifies the typical distance between two different irregularities (or bumps) on the surface. Beyond this distance, the heights are not correlated. The power spectrum density (PSD) function that can be directly obtained from AFM measurements is just the Fourier transform of $C(y)$.

Although the Gaussian correlation has been used by many authors, most of the natural surfaces present many lateral length scales. Often found in the literature is the correlation function defined by

$$C(y) = \sigma^2 \exp\{-(y - y_0)^{2H}/L^{2H}\} \quad (3)$$

with $0 < H \leq 1$.

The Hurst exponent H describes the height fluctuations on the surface: small H values specify very rough surfaces, while if H is close to 1, the surface is more regular. The fractal dimension is $3 - H$, and if $H = 1$, the fractal dimension of the interface is 2 (it equals its topological dimension) and the interface has a non-fractal (Gaussian) nature. Non-Gaussian distributed surfaces have also been studied, mainly within the framework of scattering from the ocean. The mechanism for surface generation is then more complicated.

The physical model describing the growth of multiple QD ensembles was employed as a basis for development of a structural model of a growing In(Ga)As/GaAs superlattice with pyramid-shaped InAs QDs (triangles in the plane) and the corresponding face slope [22]. It was shown also that in perfect crystalline structures with vertically correlated QD ensembles there is an additional long-range QD ordering on lateral planes which gives rise to corrugation of crystalline planes and results in a quasi-periodical distribution of the elastic deformation and QDs [23]. To rigorously include the quasi-periodicity of QD ensembles in diffraction calculations, the author used the model in which the rough surface is represented by a grating, with the large period d containing a few or a large number of quasi-random nano-ripples. In this model, the QDs lie in the lateral (growth) plane, they are, on the average, ordered, and have the same average step determined by the growth density. We shall assume for the sake of simplicity that random displacements of the QDs from their average positions are not correlated, and that displacement dispersions, QD sizes, and average QD separations in each period are the same. The degree of vertical correlation can be varied by displacing laterally one boundary relative to another or by adjusting properly the sets of displacements, sizes, and average separations between the QDs for different boundaries with the same period. By setting properly different values of the period, QD displacement dispersion, and average QD separation, as well as the QD heights and widths (or face slopes), one can model the variation of the horizontal and vertical correlations in the structural parameter of QDs. This model permits one also to specify corrugated interfaces on which QDs are arranged as quasi-periodic irregularities.

In order to compute the scattering properties of a rough surface using a forward electromagnetic solver, an ensemble of surface realizations must be generated. There exist several ways to generate rough surfaces with Gaussian height or any other structural parameter distribution and a given correlation function. The most common approach consists in generating surface profiles by a Monte Carlo procedure. A sequence of random numbers ($\sim 100,000$) with Normal statistics, zero mean, and variance $\sigma = 1$ is constructed from another random series directly generated by a computer. Then the former sequence is scaled in order to obtain a desired σ and, further, correlation with the Gaussian is performed in order to obtain a profile with a Gaussian correlation function. This is known as the spectral method [5] and used in PCGrate v.6.2. Note also that measurements of scattered light have mostly been obtained at short X-ray wavelengths and grazing angles of incidence with a slit-shaped detector. If a two-dimensional surface structure is uniform then the one-dimensional PSD of the one-dimensional grating-like structure is suitable to calculate the intensity scattered into a slit-shaped detector. For this geometry, the scattering angle changes with the position on the detector slit, and one has to integrate the differential reflectivity distribution function over all these positions or spatial frequencies, which will result in some smoothing [24].

3. APPROXIMATE METHODS FOR ROUGHNESS ACCOUNTING IN X-RAY–VUV RANGES

Scattering from rough surfaces significantly alters the power distribution between the reflected and transmitted specular fields and generates additional losses due to absorption within the multilayer film. This is a purely dynamical effect

requiring rigorous theory to correctly describe the power change in the specular order and to give the nonspecular distribution. The existing theoretical frameworks exploit the fact that interaction between X rays and matter is typically weak (“small roughness approximation”) or, alternatively, the surface is very rough whose typical length scales are much greater than the wavelength. In the first case, one treats the specular and nonspecular scattering from interfacial roughness using first-or, at most, second-order perturbation theory. Hence the theory is limited to the case where the nonspecular scattered power is small compared to the incident power. In the second case of the geometrical optics approximation (scalar theory), one launches a large number of parallel incident rays on the surface, hence polarization and resonance effects in this model are non-accountable. Despite the considerable progress attained in the last decade in developing a rigorous theory of X-ray scattering from rough multilayer films, the author is aware only of approximated and asymptotic approaches. Even a general second-order theory of scattering from 1-D rough multilayers has not yet been developed.

Within the context of the geometrical optics theory (or the high-frequency Kirchhoff integral approximation), each ray undergoes a series of reflections off the surface until it finally escapes [25]. A fundamental constraint on the application of this approach to bulk and multilayer X-ray structures, as well as to those with one dielectric coating, is imposed by the large slopes and oblique angle of incidence, which should not be extremely grazing [10]. The critical value of the angle depends, however, on the actual surface parameters and the light wavelength and polarization. The limitation on the angle of incidence is connected with the difference in scattering between the finitely and perfectly conducting bulk rough structures operating in the X-ray range under grazing incidence, particularly in the case of the TM polarization. The same applies to multilayers if the radiation penetrates all the way down to the substrate.

Within the context of perturbation theory, two different formulations are basically used in X-ray–EUV, each valid in its specific regime. The Born approximation (BA) is based on iterative solution of a volume integral equation and was first applied to homogeneous rough surfaces in the context of X-ray and neutron scattering [25]. BA refers to a family of methods in which the unknown field satisfies an integral equation of second kind, with a ‘potential’ term and a Green’s function in the integrand. The solution can then formally be expressed as an iteration series (the so-called Born or Neumann series) with the potential used as a small parameter [10]. The Born approximation usually corresponds to the first iteration. The small parameter of this expansion is typically the electric permittivity contrast, which is very small in the X-ray and EUV range. The main weakness of the BA is that it does not take properly into account the refraction by the surface and therefore fails as one approaches the so-called critical angle, at which total external reflection occurs. The BA can be improved considerably in this respect by choosing a more adapted reference problem, namely, the flat surface between two media. In this case, the free-space Green function is replaced by a half-space Green function, that depends explicitly on the Fresnel reflection coefficient at the plane interface. This is the so-called distorted-wave Born approximation (DWBA), a method which draws, as the BA, from quantum mechanics and was developed in the eighties of the last century for X-ray scattering from rough surfaces [25].

To take border roughness (or diffusion between materials of the layers) into account, we use in PCGrate v.6.1 a model based on Debye theory for the Normal law of the micro-roughness and/or interdiffusion height distribution. In this model, the effect of imperfect plane boundaries can be incorporated into efficiency calculations by describing the reduction of the reflected specular (coherent) amplitude at each boundary by the factor of the Debye-Waller model [26]

$$\exp(-2(2\pi\sigma\sin(\zeta)/\lambda)^2), \quad (4)$$

where λ is the wavelength in vacuum and ζ is the grazing angle of incidence on the plane that must be large and far from the critical angle.

The Nevot-Croce model, which can be derived from the first order DWBA, is used mostly at grazing incidence near the critical angle

$$\exp\{-2(2\pi\sigma_{l+1}/\lambda)^2 n_l \sin(\zeta_l) n_{l+1} \sin(\zeta_{l+1})\}, \quad (5)$$

where ζ_l is the grazing angle of incidence and n_l is the refractive index in layer l .

Both descriptions of the reduction of specular reflectance are valid, strictly speaking, in the case of small roughness heights and big (Eq. 4) or very small (Eq. 5) correlation lengths. It was shown [27] that the correlation function, which determines the properties of scattering from shallow microrough surfaces, becomes no longer adequate for description of the speckle pattern after the mean height of irregularities h has exceeded one-tenth of the wavelength. The use of Eqs. (4)-(5) or even more complicated approximations in the intermediate incident angle range, for high conducting surfaces, and especially in the TM polarization is also very questionable.

4. TWO RIGOROUS SOLVERS OF PCGRATE V.6.2

PCGrate-S(X) v.6.2 series software enables high-speed calculation of both multilayer resonance and small wavelength-to-period ratio cases using one of the two independent solvers, i.e. *Penetrating* and *Separating*. The solvers operate differently and behave in a mutually complementary way when applied to such difficult cases as coated gratings with thin layers, rough gratings or mirrors, and photonic crystals.

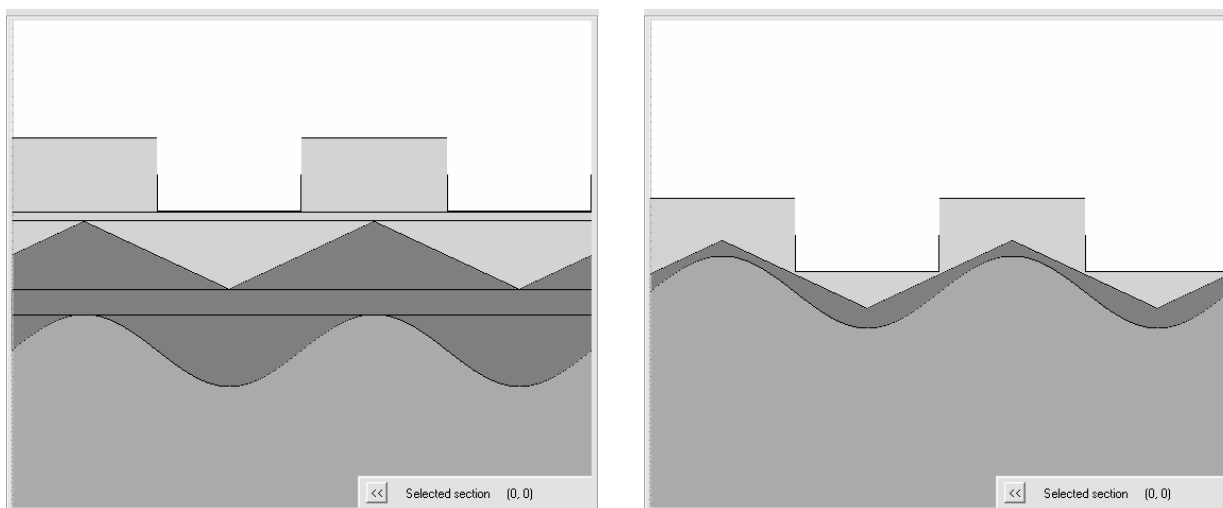


Fig.1. A multi-boundary grating model with plain gaps between two adjacent corrugated regions (left); and a multi-boundary grating model which can be calculated with the Penetrating solver only (right).

The PCGrate 6.2 *Separating* solver is based on the newly developed single-boundary integral-equation Scattering solver and the Scattering-matrix approach to multilayer diffraction [4, 6-7]. By definition, it requires that a homogeneous medium separate two adjacent corrugated regions by fictitious planes (see Fig. 1, left). The distance between such planes may be arbitrary, including very nearly zero separation. The *Separating* solver offers a fast solution to multistack problems with plane and/or conformal (obtained by a vertical translation) layers using the same solution of integral equations on a single boundary. This grating model may conveniently be illustrated by a profile of an arbitrary outline with several absolutely plane interfaces above and/or below it. Since the fields at the adjacent plane interfaces are coupled by known Fresnel coefficients, the whole multi-boundary problem can be effectively reduced to solution of integral equations on the corrugated boundary profiles only. The *Separating* solver is primarily intended for efficiency calculations for any uncoated, including rough, grating, specific types of coated gratings, and photonic crystals. It is indispensable for X-ray-VUV gratings and mirrors covered with one or many plane or rather thick conformal coatings and, especially, for grazing incidence structures.

The recently refined PCGrate 6.2 *Penetrating* solver is based on the multi-boundary marching scheme [11, 15]; it does not require separation between two adjacent corrugated regions (see Fig. 1, right). This is vital for the modeling of many coated gratings (echelles, multilayer X-ray-EUV, thin-oxidized, etc.). Therefore, the *Penetrating* solver is more general in this sense. As a rule, the *Penetrating* solver takes up more computing time than the *Separating* one to solve

such problems, because it considers an absolutely plane border as a corrugated boundary and solves integral equations on each physical boundary (it also depends on the number of the +/- terms/orders taken into account).

The PCGrate-SX 6.2 calculation solvers work reliably and very fast for very low λ or λ/d in the X-ray–EUV range, despite the small number N of collocation points per wavelength used in the MIM (it is also true for the echelles). For example, if a period includes 50 collocation points and $\lambda/d = 0.001$, there is only 0.05 point per wavelength. In this case, however, the profile depth, the bi-layer thickness, and the incident radiation wavelength must be of the same order of magnitude. The same rule for reaching the maximum diffraction efficiency is, on the whole, valid for longer wavelengths too.

5. EXAMPLES OF EXACT ACCOUNTING OF DIFFERENT-TYPES OF IRREGULARITIES

In this Section, we are going to consider examples of exact accounting of radiation scattering from irregularities of various types, more specifically, random roughness of the gold mirror illuminated by hard X-ray radiation at grazing angles, random roughness on the boundaries of a 20-bilayer Mo/Si normal-incidence grating operating in the EUV range, and quasi-periodic tenfold-multiplied In(Ga)As QD ensembles, with vertical correlation and without it, illuminated by X-rays at grazing incidence. These examples were chosen so as to permit us, in addition to checking the validity of the method in studies of nano-irregularities of any kind, to treat different wavelength ranges and specific conditions of irradiation, as well as perform comparison with approximate models and measurements. The computations were carried out with PCGrate-SX v.6.2, and in the cases of exact accounting of irregularities we conducted statistical averaging of data with a Gaussian height distribution and different correlation lengths.

5.1 A rough gold mirror

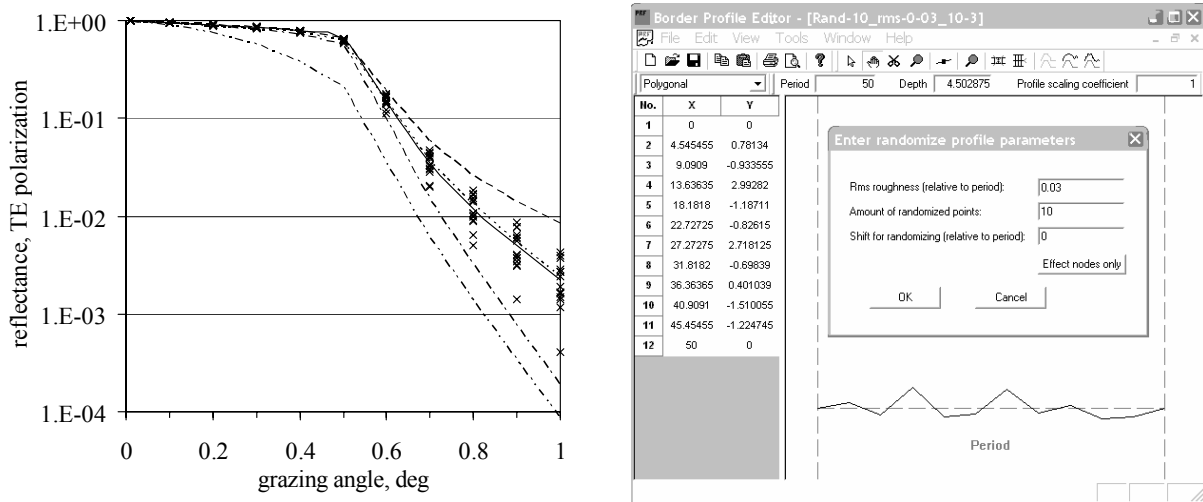


Fig. 2. (left) Calculated specular TE reflectance of gold mirror for Cu $K\alpha_1$ radiation plotted vs. angle of grazing incidence for different σ (rms roughness) and L (correlation width): $\sigma = 0$ and $L = \infty$ (long-dashed line – perfect surface); $\sigma = 1.5$ nm and $L = \infty$ (long-two-short-dashed line – Debye-Waller appr.); $\sigma = 1.5$ nm and $L = 0$ (long-short-dashed line – Nénot-Croce appr.); $\sigma = 1.5$ nm and $L = 5$ nm (data markers – rigorous model for different samples). $\sigma = 1.5$ nm and $L = 5$ nm (short-dashed line – rigorous average model for 10 samples); $\sigma = 1.5$ nm and $L = 5$ nm (solid line – rigorous average model for 15 samples). (right) A border profile sample with a 50-nm period and 10 random asperities used in rigorous models of gold X-ray mirror.

A bulk model of a typical gold X-ray mirror for use at grazing incidence near the angle of total external reflection was chosen as a starting point for the investigation. The difference between the two approximate and the rigorous approach can be clearly seen in Fig. 3 (left) which plots the calculated specular TE reflectivity of a gold mirror with rms roughness $\sigma = 1.5$ nm vs. ζ for Cu $K\alpha_1$ radiation ($\lambda = 0.1541$ nm) and for different values of the lateral correlation length L . For the Debye-Waller model $L = \infty$, for the Nénot-Croce model $L = 0$, and for statistical average rigorous

calculations, $L = 5$ nm. Thus the lateral correlation length chosen for the rigorous model is close to the one used with the Névot-Croce model. A typical border profile used for modeling of such quasi-gratings, which have an average period of 50 nm, 10 asperities, and height in the range from 3 nm to 15 nm, is demonstrated in Fig. 2 (right). Thus, the h/λ ratio may reach 100, a figure very large for any numerical method.

The results of calculation of the specular scattering component in this unfavorable example start to converge for $N > 1000$ for both solvers, and stable results with an accuracy of $1.e-5$ – $1.e-6$, as estimated from the energy balance with due accounting of finite conductivity of the material, can be obtained for $N \sim 2000$. The statistical averaging has been performed for 10 and 15 samples and the difference between the two data series, as seen from Fig. 2 (left), is about several percent. For the sake of simplicity, an equal step between randomized points is used in the calculations, which results in a fixed width of asperities; it can be changed, however, by varying the groove period statistically (see Section 2 about QD structural models). The refractive indices of gold were taken from [28].

The difference between the rigorously and approximately calculated examples is about an order of magnitude in the low reflectance range and about a few times in the intermediate range. In the high reflectance range, as well as for $\sigma = 0.15$ nm and, especially, for $\sigma = 0.015$ nm (both data series are not presented), the difference between the rigorous and Névot-Croce models is much smaller. As one can readily see from Fig. 2 (left), the rigorously calculated specular reflectances lie between the estimates made with the Névot-Croce model and those for a perfect (non-rough) mirror; this implies that the Névot-Croce factor overestimates the influence of roughness, and that the roughness values obtained by fitting experimental data to the Névot-Croce approximations are too small for grazing angles higher than the critical angle. This conclusion can be drawn also from the validity range derived for the Névot-Croce factor and for the first- and second-order DWBA theory [25].

Four complex matrices with total 8,000 unknowns were used in the Separating solver for each random sample of this problem. The time required to calculate one specular reflectance for such model (with the energy balance error of $1.e-5$) was about one hour when using all convergence accelerating options [18] and a workstation with two Intel® Pentium® 2 GHz processors, 2 Mbyte cache, 400 MHz bus clock, 2 Gbyte RAM and controlled by OS Windows® XP Pro.

5.2 A rough Mo/Si multilayer grating

The EUV normal-incidence imaging spectrometer developed for the Hinode, formerly known as Solar B [29], mission is an orbital instrument making use of a multilayer diffraction grating, and the Mo/Si coating was chosen and optimized for its optics. The toroidal diffraction grating, 100 mm in diameter and with a nominal radius of 1.18 m, having 4200 grooves/mm and rectangular (trapezoidal) groove profile of nominal depth 58 Å, was fabricated holographically by Zeiss Laser Optics GmbH, with subsequent ion etching of the fused silica substrate [15]. Different Mo/Si coatings, optimized for operation in two narrow EUV wave bands (17–21 and 25–29 nm) containing many emission spectral lines were deposited onto the two halves of the grating.

The measurements of the flight FL1 grating were performed at the Naval Research Laboratory synchrotron beamline [15]. The efficiency was measured at 60 points of a square grid covering both parts of the working grating surface 90 mm in diameter. The efficiencies of the multilayer diffraction grating were measured at nine wavelengths with the radiation incident at an angle of 6.5° to the normal on the short-band side (from 17.1 to 22.0 nm) of the grating. Except for several extreme points at the edges of the working aperture, the efficiency was found to be quite uniform over the grating surface. The efficiencies of the FL1 grating measured at the central point of its short-wavelength side (gravitation center) are identified by markers in Fig. 3 (left).

The theoretical diffraction efficiency was determined for unpolarized incidence radiation using the *Penetrating* solver and border randomizing procedure. For the short-band half of the diffraction grating, the multilayer stack parameters are 20 Mo/Si layer pairs with a bilayer period $D = 10.3$ nm and a Mo thickness-to-bilayer-period ratio $\Gamma = 0.37$, 0.2 nm Si-Mo interface rms roughness, and 0.85 nm Mo-Si rms roughness. The Si protective capping layer is 2 nm thick. The AFM-measured groove profile has the trapezoidal shape with a depth of ~ 6 nm and the slope angle of $\sim 35^\circ$. The boundary profile was assumed the same for all layers and 98 random asperities on each border were generated without a vertical correlation between borders and using the lateral correlation length $L = 2.4$ nm. The modeling was carried out using the refractive index data for Si and Mo taken from different sources [15]. There were no free parameters in the

calculation. The calculations show that only one set of 41 random borders is enough for the accurate averaging of the efficiency. A sketch of the FL1 multilayer grating is shown in Fig. 3 (right).

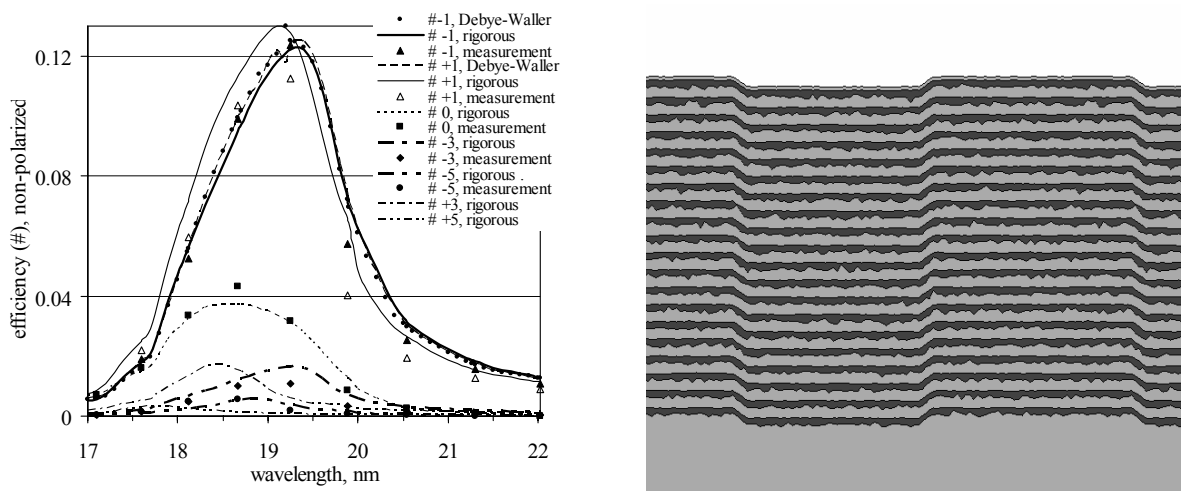


Figure 3. (left) Calculated and measured non-polarized efficiencies in plus and minus orders of the Hinode flight 4200 grooves/mm grating with 20 Mo/Si bilayers on Si and interface rms roughnesses of 0.2 nm (Si-Mo) & 0.85 nm (Mo-Si) operating at an angle of incidence of 6.5° vs. wavelength. (right) A sketch of the FL1 rough multilayer grating with a lateral correlation length L of 2.4 nm.

Figure 3 (left) indicates good agreement between the measured and rigorously calculated diffraction efficiencies of the FL1 grating in the ± 1 , 0, -3, and -5 orders over the entire working wavelength range. The product of the multilayer mirror reflectance reduced by the Debye-Waller factor by the grating relative efficiency, which was used in the approximate model to account for the layer interdiffusion and random microroughness [15], is shown for comparison in the same figure. As was discovered and described by Seely *et al.* [30], while the physical model based on accounting of the Debye-Waller factor does not yield wavelength separation of the inside and outside orders, this model is capable of accurately predicting for this particular groove profile the shape of the efficiency curves and the heights of their maxima. The above model based on rigorous accounting of random border roughness not only yields separation of efficiency curves in the plus and minus orders in wavelength but predicts also exactly the absolute efficiencies reduced as a result of scattering from asperities. Because the heights of the maxima and the shapes of the efficiency curves for different orders are similar (but do not coincide!) for the rigorous and the approximate models, the effect of roughness on the decrease of specular reflectance from a plane multilayer mirror for a mean-height roughness/wavelength ratio less than ~ 0.1 and close to normal incidence can be determined by approximate techniques involving, for instance, the accounting of the Debye-Waller correction, which conforms with the estimate made for the visible and IR ranges [27].

The time required to calculate one point using a randomly-rough 41-border rigorous model for the FL1 grating (with the energy balance error of $\sim 1.e-3$) was about 7 min when using the above mentioned workstation and without using convergence accelerating options.

5.3 Multiple quantum dot ensembles

Two samples were grown by molecular beam epitaxy. Both of them consisted of 10 InAs QD sheets (two mono layers of InAs were deposited on each QD layer) separated by 10 nm and 40 nm of GaAs, thus providing vertically correlated and non-correlated QD arrays. In the former case (10 nm), the dots were perfectly aligned vertically (which is confirmed by transmission electron microscopy), in the later case they were arranged more or less randomly.

Measurements were performed on the samples using the grazing incidence X-ray diffraction techniques at a wavelength of Cu $K\alpha_1$ with a Hotbird diffractometer and a position sensitive detector [31]. The beam divergence was 0.01° and an angular resolution of 0.005° was chosen. By comparing the theoretical with experimental X-ray reflectances (Fig. 4, left), the average values of $h = 5.0$ nm and $L = 16.7$ nm determined in the Stranski-Krastanow growth model [22], as

well as the superlattice parameters, were substantiated and refined by the fitting procedure for two different samples in the range near the critical angle.

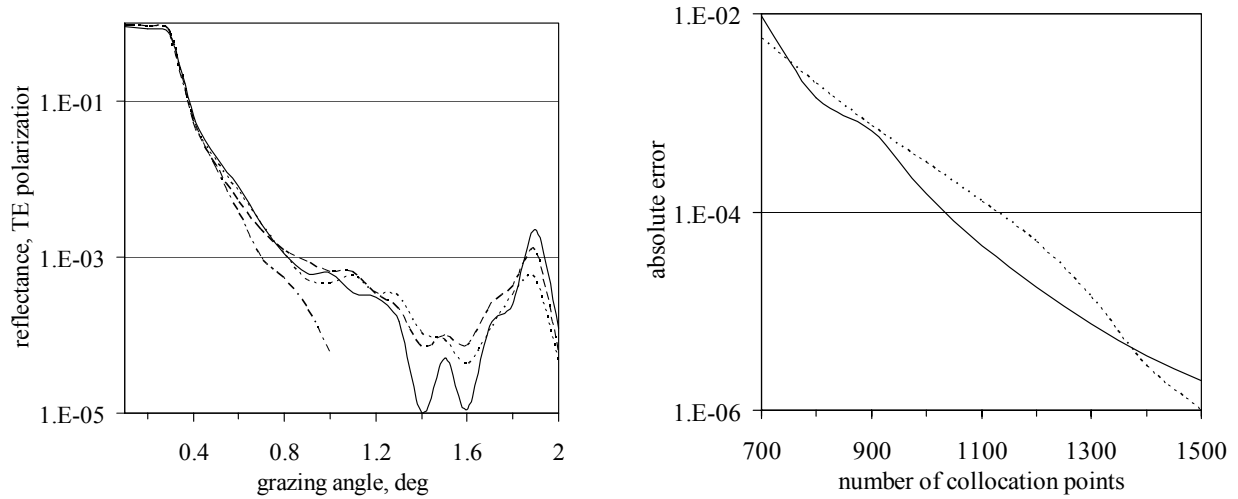


Figure 4. (left) Specular reflectance for a sample with vertically non-correlated QDs operated at 0.154-nm wavelength vs. grazing angle of incidence: perfect plane structure model (short-dashed line); Névo-Croce approximation with rms roughness of 1.45 nm for triangles (long-dashed line); rigorous calculation with QD height $h = 5$ nm and width $L = 16.7$ nm (solid line); measurement (long-short-dashed line). (right) Absolute error for energy balance (solid curve) and specular reflectance (short-dashed line) for a sample with vertically non-correlated QDs operated at 0.154-nm wavelength and 0.5° grazing incidence vs. number of collocation points

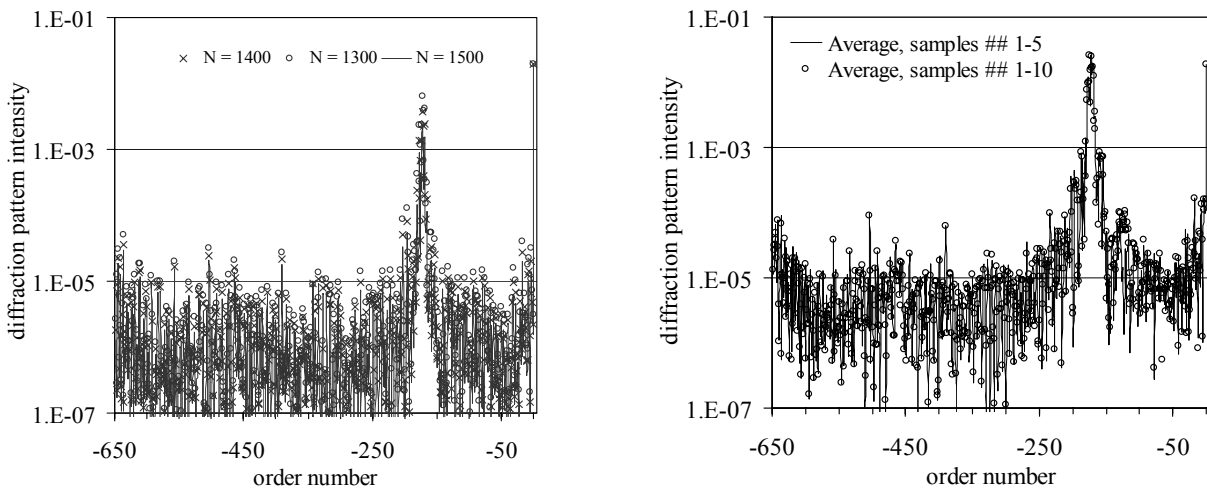


Figure 5. (left) Specular and non-specular reflectance of a statistical realization calculated with different numbers of collocation points N for a sample with vertically non-correlated QDs, 0.154-nm wavelength, and 0.5° grazing incidence vs. grazing diffraction angle (order number) in the range from -4.3° to $+0.5^\circ$. (right) Specular and non-specular reflectance of an average sample with vertically non-correlated QDs calculated for 0.154-nm wavelength and 0.5° grazing incidence vs. grazing diffraction angle (order number) in the range from -4.3° to $+0.5^\circ$. The strong diffuse peak is near the grazing diffraction angle of 61.5° (-172 order).

Both specular and nonspecular scattered intensities were theoretically determined for TE-polarized incident radiation using the *Penetrating* solver and the border randomizing procedure. The refractive indices for InAs and GaAs were taken from [28]. The convergence of the method is illustrated by a statistical realization of the geometrical parameters of

borders with vertically uncorrelated QDs and $\zeta = 0.5^\circ$ visualized in Fig. 4 (right), which plots the absolute errors of the energy balance and specular reflectance vs. N . The graphs were drawn in the log scale; for the exact value of the reflectance was taken its iterated value, the last on the axis in Fig. 4 (right). We readily see that both curves are nearly linear and close to one another, which implies a high convergence of the results and error scalability. The grazing angle of incidence of 0.5° is a difficult angle from the standpoint of attaining convergence and a high accuracy of results, because it is larger than the total external reflection angle while approaching it, and the attendant multiple and multi-wave scattering effects influence strongly the speckle intensity distribution. Figure 5 (left) demonstrates the convergence of the calculation of the diffuse scattering component as a function of N . As expected, the convergence of the calculations of nonspecular scattering intensity is much worse than that for the specular case. Nevertheless, the general trend is obvious in Fig. 5 (left), and reliable results can be reached by choosing large enough N and the required statistical averaging.

Calculations have revealed a weaker dependence of specular scattered intensities on L and a stronger one on h , a feature that is especially noticeable at high grazing angles. Also, noticeable differences appearing at these angles between the approximate (Névo-Croce model) and the rigorous methods, on the one hand, and the theory and experiment, on the other, find an adequate explanation. The angular dependences of diffuse scattering intensity exhibit very strong peaks near the angles ζ_{diff} to the surface corresponding to specular reflection from the QD facets (Fig. 5, right), the so-called blaze condition for gratings:

$$2\alpha = \zeta_{\text{diff}} - \zeta_{\text{inc}}. \quad (6)$$

where α is the facet angle of QDs ($\tan \alpha = 2h/L$). The good agreement between the results obtained from the blaze equation and those derived numerically suggests the validity of our computations and substantiates the possibility of extracting the QD slope angles from measurements of X-ray diffuse scattering. These peaks exist at nearly the same diffraction angles for QDs with the same slope angle; their intensities, however, may differ by many times for the correlated and non-correlated QD structures having the equal QD density. Such determination of the QD slope angle and of the vertical correlation rate, as well as of other structural parameters, can be performed with a high accuracy, provided the data sample to be averaged is statistically large enough. In this case, the statistical averaging was performed only for 5 and 10 generally random samples; we readily see, however, that the averaged data series do converge, in particular for even orders. This attests to the proposed approach being promising.

The time required to calculate one reflectance for all scattering angles for a 21-border QD structure (with the energy balance error of $\sim 1.e-5$) was about 3.5 hours when using the above mentioned workstation and all the convergence accelerating options.

6. CONCLUSIONS

To sum up, we are formulating now the most essential conclusions of the present study and suggest possible related directions to be pursued.

The rigorous accounting of random, periodical and quasi-periodical asperities of multilayer 1-D structures with any (Gaussian and non-Gaussian) surface statistics has been used for the first time, including calculations of diffuse X-ray scattering.

Examples of exact calculations of scattered intensities for mirrors, gratings and quasi-periodical structures like multiple QDs are presented in the wavelength range from X-ray to EUV. The convergence and accuracy of the data obtained has been estimated. The results are compared with the data obtained by the known approximation methods and derived from measurements.

The diffracted speckle pattern obtained in the X-ray–EUV range for any kind of structures having high asperities can differ from those calculated for ideal or AFM-measured average profiles (without randomization) or derived from approximations by a few percent up to orders of magnitude. Mean intensities can be obtained by averaging intensities of

a few or of a large number of statistical samples; it depends on both the structural parameters of the samples with irregularities and on the parameters of the incident radiation. For incidence, for a gold mirror with random roughness the Névo-Croce approximation yields underestimated specular reflectances for grazing angles larger than 0.5° . For a grazing angle of 1° , the approximate value is one tenth of the result obtained by averaging only 15 exactly calculated statistical data. For multilayer structures the situation becomes still more complex, and one will have to drive estimates from rigorous calculations and statistically reliable averaging.

Quantitative determination of the specular and, particularly, of nonspecular components of short-wavelength radiation scattered by asperities of multilayer structures under nearly normal incidence requires invoking rigorous numerical methods in the cases where the ratio of the mean asperity height to the wavelength is > 0.1 , which coincides with the criterion found for long-wavelength radiation and one perfectly conducting boundary [27]. As the incidence angle increases, this ratio grows to a few orders of magnitude for strongly grazing angles; it cannot be found, however, by any way other than a comparison of approximate results with accurate data or measurements. Randomly rough borders should be included in rigorous efficiency calculations by way of numerical randomization, if the statistics is known, or from a set of data samples obtained, for example, from AFM measurements.

The proposed approach to numerical treatment of X-ray diffraction from low-dimensional structures like multiple QDs permits one not only determine the specular and the diffuse reflectance component but to derive structural parameters of samples as well by fitting the experimental to theoretical scattering intensities. A theoretical study has revealed that the angular spectrum of scattering from QD ensembles should contain a resonance corresponding to specular reflection from QD faces, a point that requires experimental verification. The position of the resonance should yield the lateral width (or slope) of the QDs with a high accuracy, and its height taking into account a 2-D nature of QD structures, the degree of their vertical correlation.

The *Separating* solver based on the rigorous MIM and scattering matrix approach is added to the improved *Penetrating* solver of PCGrate-SX v.6.2 to expand the range of solvable problems and to speed up by orders of magnitude the cumbersome computations similar to those presented in this report. Despite the Moor's law and the remarkable progress reached in computer technologies, the problems involved are among the most difficult ones encountered in numerical computational applications, both because of a very poor convergence of rigorous methods employed in short-wavelength (high frequency) problems and as a result of their being of a purely statistical nature. Both these reasons stress the need for further refinement of the rigorous methods and the corresponding programs and carrying out time-consuming computations.

ACKNOWLEDGMENTS

The author feels indebted to S. Yu. Sadov for the information provided and fruitful discussions. Partial support of the Russian Foundation for Basic Research and Quantum Nanostructures Scientific Program of the Russian Academy of Sciences is gratefully acknowledged.

REFERENCES

1. R. Petit, ed., *Electromagnetic Theory of Gratings*, Springer-Verlag, Berlin, 1980.
2. D. R. Maystre, ed., *Diffraction Gratings*, SPIE Optical Engineering Press, Bellingham, 1993.
3. K. F. Warnick and W. C. Chew, "Rigorous solutions for electromagnetic scattering from rough surfaces," *Waves Random Media* 11(1), R1-R30 (2001).
4. L. Li, "Formulation and comparison of two recursive matrix algorithms for modeling layered diffraction gratings," *J. Opt. Soc. Am. A* 13(5), 1024-1035 (1996).
5. L. Tsang, J. A. Kong, K.-H. Ding, and C. O. Ao, *Scattering of Electromagnetics Waves: Numerical Simulations*, Wiley, 2001.
6. M. Neviere and E. Popov, *Light Propagation in Periodic Media: Differential Theory and Design*, Marcel Dekker, New York, 2002.

7. D. Maystre, "Electromagnetic study of photonic band gaps," *Pure Appl. Opt.* 3, 975-993 (1994).
8. B. H. Kleemann, A. Mitreiter, and F. Wyrowski, "Integral equation method with parametrization of grating profile: theory and experiments," *J. Mod. Opt.* 43(7), 1323-1349 (1996).
9. L. I. Goray, "Modified integral method for weak convergence problems of light scattering on relief grating," *SPIE Proc.* 4291, 1-12 (2001).
10. L. I. Goray, "Numerical analysis of the efficiency of multilayer-coated gratings using integral method," *Nuclear Inst. and Methods in Physics Research A* 536(1-2), 211-221 (2005).
11. L. I. Goray, I. G. Kuznetsov, S. Yu. Sadov, and D. A. Content, "Multilayer resonant subwavelength gratings: effects of waveguide modes and real groove profiles," *J. Opt. Soc. Am A* 23(1), 155-165 (2006).
12. N. Dechamps, N. de Beaucoudrey, C. Bourlier, and S. Toutain, "Fast numerical method for electromagnetic scattering by rough layered interfaces: Propagation-inside-layer expansion method," *J. Opt. Soc. Am. A* 23(2), 359-369 (2006).
13. E. G. Loewen, and E. Popov, *Diffraction Gratings and Applications*, Marcel Dekker, New York, 1997.
14. M. Saillard and A. Sentenac, "Rigorous solutions for electromagnetic scattering from rough surfaces," *Waves Random Media* 11(3), R103-R137 (2001).
15. L. I. Goray, J. F. Seely, and S. Yu. Sadov, "Spectral separation of the efficiencies of the inside and outside orders of soft-x-ray-extreme-ultraviolet gratings at near normal incidence," *J. Appl. Phys.* 100(9), 094901-1-13. (2006).
16. A. Rathsfeld, G. Schmidt, and B. H. Kleemann, "On a Fast Integral Equation Method for Diffraction Gratings," *Commun. Comput. Phys.* 1(6), 984-1009 (2006).
17. Web site, <http://www.pcgrate.com>
18. L. I. Goray and S. Yu. Sadov, "Numerical modelling of coated gratings in sensitive cases," *OSA DOMO* 75, 365-379 (2002).
19. D. A. Content, P. Arsenovic, I. G. Kuznetsov, and T. Hadjimichael, "Grating groove metrology and efficiency predictions from the soft x-ray to the far infrared," *SPIE Proc.* 4485, 405-416 (2001).
20. L. I. Goray and J. F. Seely, "Efficiencies of master, replica, and multilayer gratings for the soft x-ray - EUV range: modeling based on the modified integral method and comparisons to measurements," *Appl. Opt.* 41(7), 1434-1445 (2002).
21. I. Kegel, T. H. Metzger, A. Lorke, J. Peisl, J. Stangl, G. Bauer, J. M. Garcia and P. M. Petroff, "Nanometer-Scale Resolution of Strain and Interdiffusion in Self-Assembled InAs_GaAs Quantum Dots," *Phys. Rev. Lett.* 85(8), 1694-1697 (2000).
22. V. G. Dubrovski, G. E. Cirilin, Yu. G. Musikhin, Yu. B. Samsonenko, A. A. Tonkikh, N. K. Polyakov, V. A. Egorov, A. F. Tsatsul'nikov, N. A. Krizhanovskaya, V. M. Ustinov, and P. Werner, "Effects of growth kinetics on the structural and optical properties of quantum dot ensembles," *J. Cryst. Growth* 267, 47-59 (2004).
23. N. N. Faleev, A. Yu. Egorov, A. E. Zhukov, A. R. Kovsh, S. S. Mikhrin, V. M. Ustinov, K. M. Pavlov, V. I. Punegov, M. Tabuchi, and Y. Takeda, "X-Ray diffraction analysis of multilayer InAs/GaAs heterostructures with InAs quantum dots," *Semiconductors* 33(11), 1229-1237 (1999).
24. E. Spiller, *Soft X-ray Optics*, SPIE Press, Bellingham, Washington, 1994.
25. T. M. Elfouhaily and C.-A. Guerin, "A critical survey of approximate scattering wave theories from random rough surfaces," *Waves Random Media* 14(1), R1-R40 (2004).
26. D. G. Stearns, D. P. Gaines, D. W. Sweeney, and E. M. Gullikson, "Nonspecular x-ray scattering in a multilayer-coated imaging system," *J. Appl. Phys.* 84(2), 1003-1028 (1998).
27. M. Saillard, D. Maystre, and J. P. Rossi, "Microrough surfaces: influence of the correlation function on the speckle pattern," *Optica Acta* 33(9), 1193-1206 (1986).
28. Web site, http://www.cxro.lbl.gov/optical_constants/getdb2.html
29. Web site, <http://solarb.msfc.nasa.gov/>
30. J. F. Seely, L. I. Goray, D. L. Windt, B. Kjornrattanawanich, Yu. A. Uspenskii, and A. V. Vinogradov, "Extreme ultraviolet optical constants for the design and fabrication of multilayer gratings," *SPIE Proc.* 5538, 43-52 (2004).
31. L. I. Goray, G. E. Cirilin, E. Alves, Yu. B. Samsonenko, A. A. Tonkih, N. K. Polyakov, V. A. Egorov, "Determination of the structural properties of multiple quantum dot ensembles based on a rigorous X-ray specular and diffuse scattering analysis and comparison with measurements," in 15th Int. Symp. *Nanostructures: Physics and Technology*, Novosibirsk, Russia, June 25-29, 2007.